

Rotor Wake/Stator Broadband Noise Calculations Using Hybrid RANS/LES and Chorochronic Buffer Zones

Martin Olausson* and Lars-Erik Eriksson†

Chalmers University of Technology, SE-412 96 Gothenburg, Sweden

The interaction between rotor wake turbulence and stators is a major source of fan broadband noise. This paper presents a method on how to obtain the low to medium frequencies using a hybrid RANS/LES method. Three stator vanes are discretized and the mean rotor wake is specified at the inlet. Synthetic fluctuations are also added to the inlet profile to trigger the flow into turbulent mode. Chorochronic periodic boundary conditions combined with temporally damped buffer zones (chorochronic buffer zones) are used to make sure that the deterministic part of the wake interaction is taken care of properly. The combination of chorochronic periodicity and buffer zones in the area close to the pitch-wise boundaries efficiently filters the flow field from turbulence generated stochastic fluctuations. The center blade in the domain is relatively unaffected by the filtering effect and the unsteady pressure field, deterministic and turbulence generated, can be used as a source for both tone and broadband noise. The paper also include a comparison between the proposed method and a simulation with modified blade count and standard periodic boundaries. The tone noise will change when the number of blades is modified but the aim is to see whether this has a significant effect on broadband noise.

Nomenclature

Roman

R Radial coordinate

x Axial coordinate

Greek

θ Tangential coordinate

ϕ Fourier coefficients of state vector

Subscript

n Harmonic number

Abbreviations

BPF Blade Passing Frequency

CAA Computational Aeroacoustics

CFD Computational Fluid Dynamics

FFT Fast Fourier Transform

FWH Ffowcs Williams-Hawkings

LES Large Eddy Simulation

RANS Reynolds Average Navier Stokes

*PhD student, Division of Fluid Dynamics, Department of Applied Mechanics, Chalmers University of Technology, SE-412 96 Göteborg, Sweden.

†Professor, Division of Fluid Dynamics, Department of Applied Mechanics, Chalmers University of Technology, SE-412 96 Göteborg, Sweden.

I. Introduction

Aeroengine noise has been a growing concern during the last half century and it has been regarded as a health problem for people living in the vicinity of airports. A lot of effort has been put down on reducing the noise and an important part of this process is to predict it accurately. The noise from subsonic jets has recently been accurately predicted using a combination of large eddy simulations (LES) and computational aeroacoustics (CAA).¹⁻³ This kind of jet noise is mainly produced by turbulence from the mixing process and it is of broadband character. As the bypass ratio of new engines increase the fan noise becomes a greater challenge.⁴ The rotor alone generate noise but this work only concerns the interaction between rotor wakes and stators. The interaction noise consists of a tonal part that mainly depends on the mean rotor wake impingement on the stators, the rotor speed and blade counts. It also consist of a broadband part that is produced when the turbulence in the rotor wake hit the stators. Tone noise follows the theory of Tyler and Sofrin and can be predicted using unsteady Reynolds averaged Navier-Stokes (URANS) chorochronic methods or linearized methods where the mean part of the rotor wake interact with the stators.⁵⁻¹³ These methods can with todays computational capabilities be used on industrially relevant problems since the periodicity of the blades can be utilized and only one passage needs to be discretized. The next big obstacle is to predict the broadband interaction noise that is not deterministic in the same way as the tonal part. A lot of work focuses on predicting the broadband noise from turbulence data whereas this paper aims at resolving as much of the turbulence in the rotor wake as possible.^{4,14} Some work has been initiated to address such a method and it will require not only an LES-like computation to capture the turbulent fluctuations but also a full 360° computational domain to account for all non-periodic behavior in the flow.^{15,16} This would be an impractically large task with todays computational power, at least for the fan stage in a modern high bypass ratio turbofan engine. This paper presents a mix between the tonal URANS chorochronic method and a 360° LES computation. The low to medium frequencies can be captured if three stator vane passages are discretized and a method based on hybrid RANS/LES and chorochronic buffer zones, periodic chorochronic boundaries combined with temporally damped zone, are used.

II. Methodology

The mean rotor wakes are specified at the inlet of the domain that contains the three stator vane passages and the wakes will have some distance to evolve, become turbulent, before they hit the stators. The center vane is relatively unaffected by the filtering effect that the chorochronic periodic boundaries and buffer zones has on the flow. The pressure fluctuations on the center vane can therefore be used as a source for both tone and broadband noise, since the resolved turbulent structures will result in pressure fluctuations on the vane with other frequencies than those of the mean wake blade passing frequency and harmonics of it.

II.A. Chorochronic periodicity

The interaction between two arbitrary sets of blade rows that are rotating with different angular velocities can be computed by using chorochronic boundary conditions, also known as the “shape correction method”.^{6-11,17} Only one blade per blade row needs to be discretized to capture the Tyler and Sofrin interaction modes, i.e. tone noise. The broadband noise on the other hand will include other frequencies and other modes compared to the deterministic part, hence the use of a few (three) passages to allow for some non-periodic behavior in the flow.

Fourier series of the flow variables at the chorochronic periodic boundaries are updated with a moving average technique.^{6,11,12,17} The Fourier coefficients are tuned for the deterministic part of the flow, i.e. mean wake interaction, and they are evaluated with a time shift and rotated to fit the condition at the other side of the pitch-wise boundaries, as shown in Figure 1. Some extra temporal damping is applied near the periodic boundaries to damp out errors that will grow and contaminate the solution otherwise.^{7,8,10-12} The temporal damping will also work as a buffer zone for the non-deterministic part of the flow. This is necessary since the turbulence and pressure fluctuations generated from it are uncorrelated between the blades, and cannot be transferred to the other side by the chorochronic periodic boundary condition. There would be unphysical reflections at the pitch-wise boundaries without buffer zones due to the stochastic variations in the flow that the Fourier coefficients in the chorochronic b.c. cannot hold. Figure 2 shows a buffer zone mesh for a case with three passages.

The chorochronic periodic boundary condition has been evaluated in several rotor wake/stator interaction

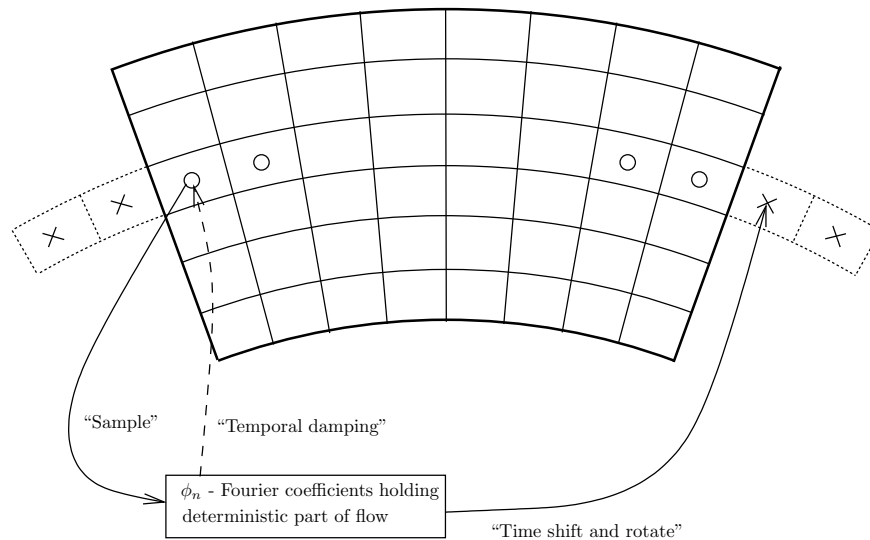


Figure 1. Simplified diagram of how the chorochronic periodic b.c. with temporal damping works. Rings represent physical cells inside the domain and crosses are ghost cells used to calculate fluxes through the boundary. The Fourier representation of the deterministic part of the flow near a boundary is updated continuously by sampling. It is used both in ghost cells at the other side of the boundary and in a temporal (chorochronic) buffer zone.

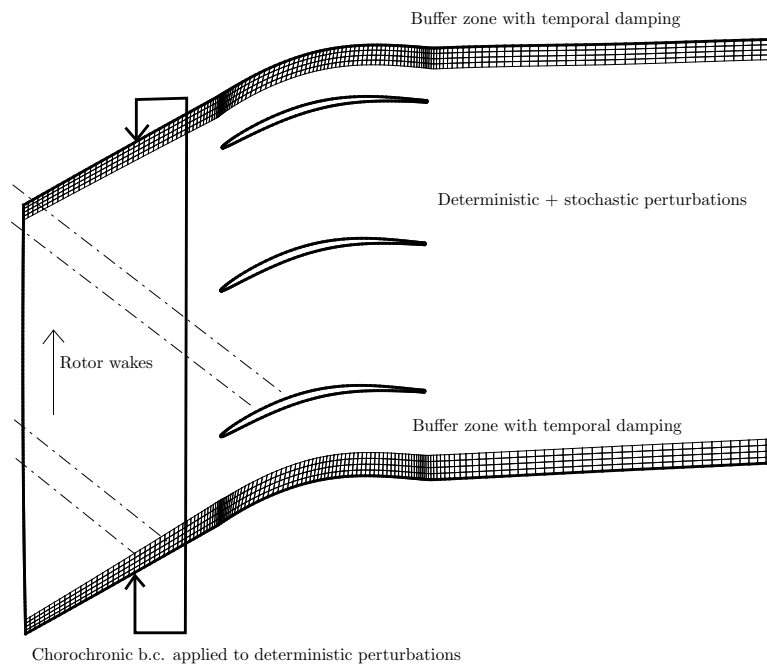


Figure 2. Mesh at mid radius close to chorochronic periodic boundaries (every other node shown). This area works as a buffer zone with temporal damping for the non-deterministic fluctuations. There are both deterministic and stochastic perturbations inside the other part of the domain, but at the pitch-wise boundaries the stochastic portion is damped out. The mean rotor wake, with synthetic fluctuations, is specified at the inlet (left side), and the chorochronic periodic b.c. is applied to the deterministic perturbations.

computations and has shown good results.^{11,12,17} It has both been compared to simple test cases where a few passages are discretized and ordinary periodic boundary conditions can be used, and also compared to a frequency domain linearized solver that has been validated against independent data.¹³

II.B. Isotropic synthetic fluctuations

The mean rotor wake is obtained from a separate steady state RANS computation in the rotor frame of reference. Isotropic synthetic fluctuations are added to the mean wake profile at the inlet to the stator domain computation to trigger the equations into turbulent mode.¹⁸ The synthetic turbulence is generated on a plane, a 2D mesh, as shown in Fig. 3 and includes fluctuations in all three space dimensions. The plane has the same length as the whole mean circumferential length of the duct and the same height as the hub to shroud distance. These fluctuations are added to the mean rotor wake profile as shown in Fig. 4. The fluctuations should rotate with the wake and therefore both the synthetic turbulence and the mean rotor wake may be decomposed into tangential modes and added together for each radial position in the mesh. The Fourier decomposed wake and the fluctuations can then easily be evaluated at different tangential positions and the result is a unique wake for each rotor blade.

The fluctuations are created from a specified length scale, taken as the width of the rotor wake, and an energy spectrum. They are kept isotropic on the entire inlet plane and are not scaled by any turbulent data from the rotor RANS computation.¹⁸

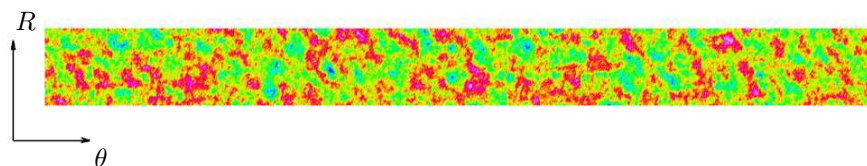


Figure 3. Synthetic fluctuations (axial velocity fluctuations are shown)

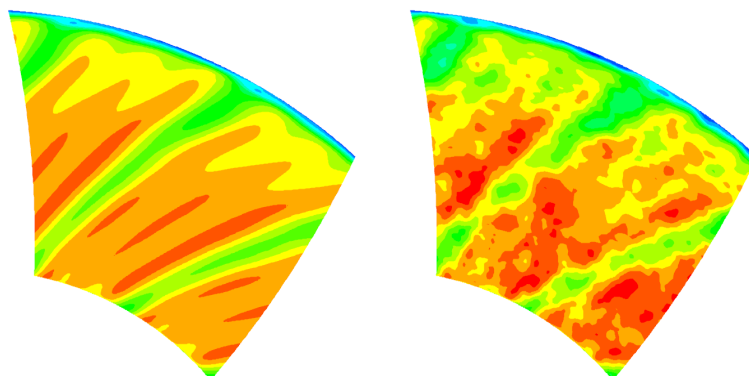


Figure 4. Axial velocity of the mean rotor wakes are shown the the left and mean rotor wakes plus synthetic fluctuations are shown to the right. The Fourier coefficients are evaluated on the inlet to the stator computational domain.

II.C. Solver

The solver, based on the G3D family of codes,¹⁹ solves the unsteady Reynolds-averaged Navier-Stokes equations with realizable $k-\varepsilon$ turbulence model, by using a finite volume solver with a low dissipation third-order upwind scheme for the convective fluxes, and a second order centered difference scheme for the diffusive fluxes. The solution is updated with a three-stage Runge-Kutta technique. The turbulent length scale in the $k-\varepsilon$ model is limited to about 20% of a typical cell size. It can be shown that the turbulence model then works as a Smagorinsky subgrid scale LES model everywhere except close to solid walls where the increased resolution result in a local URANS model.^{20,21} This type of LES flow solver has previously been successfully applied to predictions of broadband noise from subsonic jets.^{2, 3, 22, 23}

III. Results

A stator vane has been discretized with three passages as shown in Figs. 5 and 6. The mesh contains about 15M cells in total and pressure waves up to the 3rd BPF are captured with this resolution. Figure 5 shows the mesh at mid radius and Fig. 6 shows the hub and the three stator vanes surface mesh. The geometry is typical for a modern high bypass ratio fan stage. The number of stator vanes is modified into two different cases. The stator vane geometry, the rotor wake and the number of rotor blades are the same for both cases, but the number of stator vanes is modified to obtain a 2:3 blade count ratio, and thus a case with standard periodic boundary conditions. The mesh is in both cases aligned with the flow so that the rotor wakes should not pass through the periodic boundaries before they hit the stator vanes, or at least the part of the wake that impinge on the center vane. This is necessary since the synthetic fluctuations specified at the inlet do not fit the periodicity of the three stator vanes and the chorochronic periodic boundary condition will filter the flow from the stochastic perturbations.

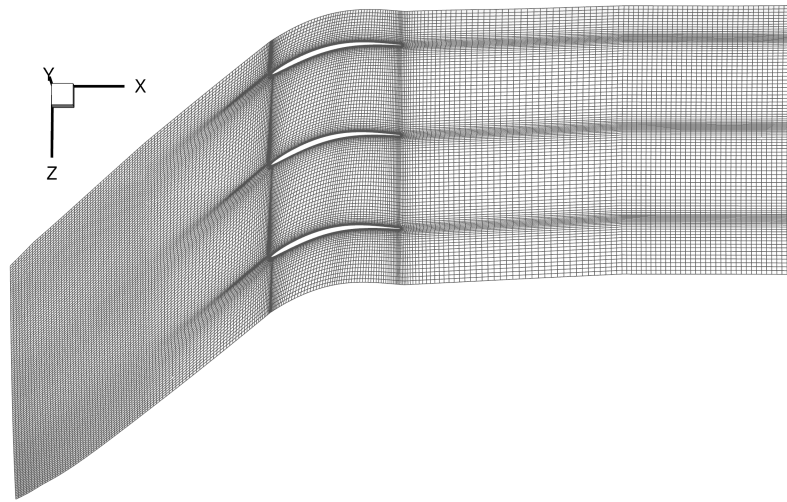


Figure 5. Mesh at mid radius (every other node shown). Flow goes from left to right, and the rotor wake is specified at the inlet. The mesh has a fine resolution at the entire inlet section to resolve turbulent fluctuations in the wake.

III.A. Case I

The number of stator vanes in case I is 1.5 times the number of rotor blades. This case serves as a reference case and standard periodic boundary conditions are used at the pitch-wise boundaries since two rotor wakes fit inside the three stator domains. There is therefore no need for a time shift in the periodic boundary. This case was first computed without any synthetic fluctuations at the inlet. The rotor wake was analyzed a bit downstream of the inlet, at a plane in front of the stator vanes, and no stochastic perturbations were identified. The shear in the mean wake specification at the inlet was not enough to trigger the equations into turbulent mode. Isotropic synthetic fluctuations were computed and added to the inlet boundary condition as described above. Figure 7 show the axial velocity component at the inlet plane and on a plane a bit downstream before the stators. It can be seen that the wakes are triggered to become turbulent.

The turbulent wake impinges on the stators and the surface pressure of the center vane, hub and shroud walls are sampled 660 times in total and at a frequency of 30 times for each rotor blade passing period. The surface pressure is then Fourier decomposed into the rotor blade passing frequency and five harmonics. This part is correlated between the vanes and is treated as tone noise. The decomposed pressure is evaluated at

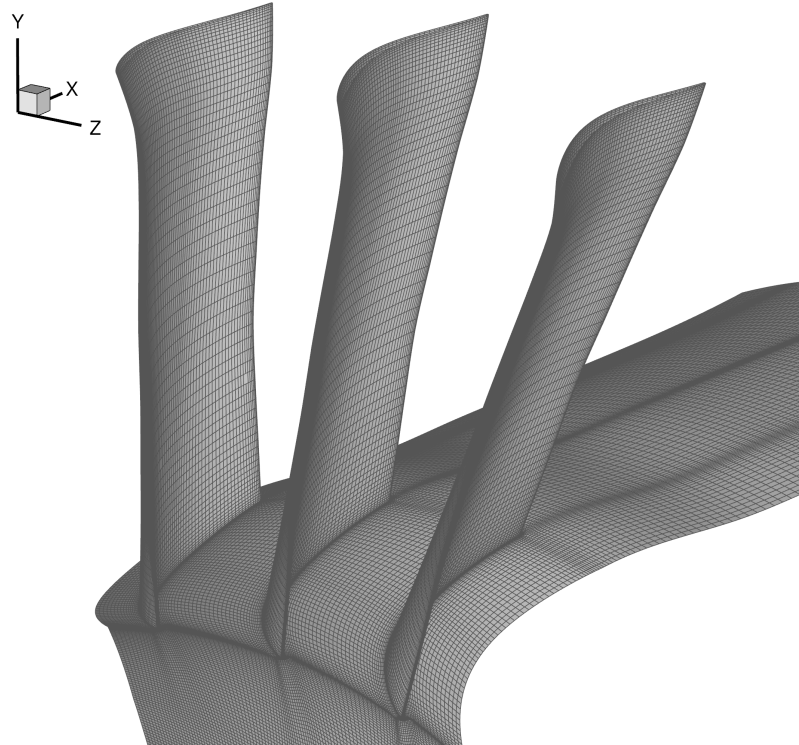


Figure 6. Stator vanes and hub Surface mesh (every other node shown). Geometry is typical for the stators in a fan stage of a modern high bypass ratio turbofan engine.

each sampling time and subtracted from the instantaneous pressure. The result is the broadband noise source and it is assumed to be uncorrelated between the vanes. An instantaneous picture of the surface pressure source for both tone and broadband noise is shown in Fig. 8, where the tone noise source is evaluated from the Fourier decomposition.

These sources are evaluated separately via a FWH surface integral method.^{24,25} The tone noise source is copied, time shifted and rotated to get the correct deterministic pressure source, i.e. the correct phase relation between the vanes. The deterministic surface pressure from all vanes are then evaluated by the FWH method and a power spectra is calculated via FFT from the observer pressure signal. The broadband source on the other hand is integrated to an observer position alone, i.e. the center vane from the computation alone is used in the surface integral. A power spectra is calculated via FFT and it is then multiplied by the number of stator vanes to get the sound power from all the vanes. This can be done since the broadband noise source is assumed to be uncorrelated between the vanes. The power spectra of broadband noise is also band-pass filtered in third octave bands since the number of samples are limited.

Figure 9 show the power spectra of tone, broadband and total noise at an observer position about one shroud diameter downstream of the vanes at the shroud radius. The ratio between tone and broadband noise is sensitive to the observer position because the propagation of the duct modes is not treated correctly. The nonzero modes of tone noise decays rapidly when the observer position is moved further away from the vanes, whereas mode zero in the third harmonic to the BPF and the broadband noise decay as normal propagating sound. Further on, the nonzero modes also decay when the observer position is moved towards the axis but at the same time mode zero grows. The broadband noise is relatively unaffected by the radial position of the observer.

The sampled surface pressure in case I has been analyzed at four points on the stator vane. Figure 10-13 show power spectra of pressure at a point on the leading edge, trailing edge, pressure side and suction side at mid radius. The figures are divided into a deterministic part, a broadband part and the total pressure. The deterministic part is obtained by a Fourier decomposition of the rotor wake BPF and harmonics, and the broadband part is the sampled pressure minus the deterministic part. The broadband surface pressure

is then also band-pass filtered in third octave bands the same way as is done for the observer pressure in Fig. 9. The total power spectra is obtained by adding the deterministic spectra to the filtered broadband spectra. Figure 14 show a log-log plot of the total pressure power spectra and it can be seen that the pressure fluctuations on the point at the leading edge is about two orders of magnitude larger than at the other points. The ratio between deterministic and stochastic fluctuations is also larger at the leading edge point compared to the other.

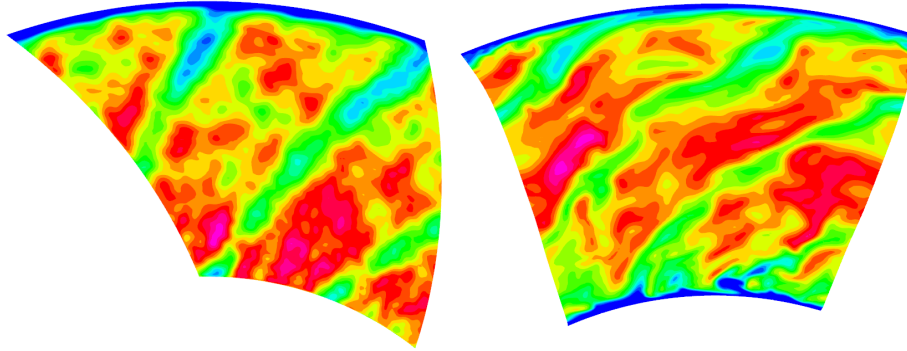


Figure 7. Axial velocity showed on a constant x plane at the inlet to the left and on a plane a bit downstream in front of the stators to the right. The synthetic fluctuations that are added at the inlet triggers the wake to become turbulent.

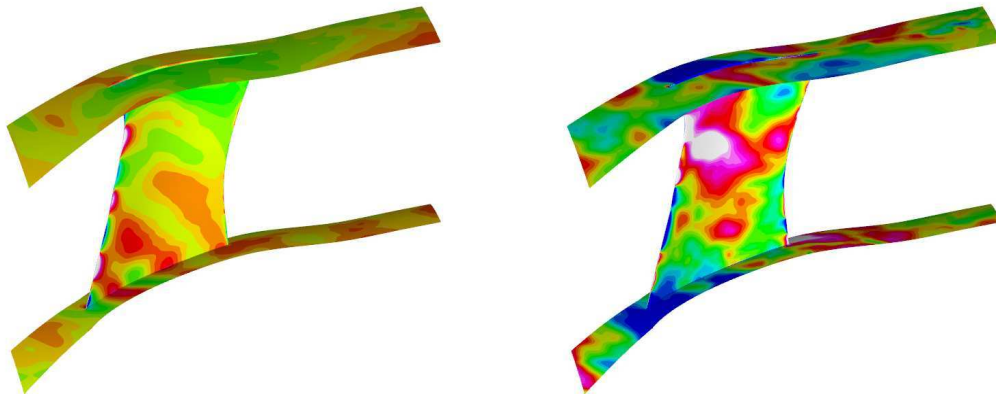


Figure 8. Instantaneous picture of deterministic surface pressure (tone noise source) is shown to the left and stochastic surface pressure (broadband noise source) is shown to the right.

III.B. Case II

The number of stators in case II is about 1.56 times the number of rotor blades. The rotor wakes do not fit inside the three stator domains and chorochronic, time lag, periodic boundaries are applied at the pitch-wise boundaries. Temporal damping is applied in the cells close to the periodic boundaries, as shown in Fig. 2. This area then works as a buffer zone for the non-deterministic fluctuations. The same wake specification, including the synthetic fluctuations, is applied at the inlet and the flow is quickly triggered into turbulent mode. The surface pressure is also sampled 660 times at the same frequency as in case I.

This is a design for low tone noise and it can be seen in the power spectra in Fig. 15 that the tone noise is lower in this case compared to case I (Fig. 9), at least for the first and second BPF. The observer position and the way that the spectra is calculated is the same as in case I. The broadband noise is similar in both

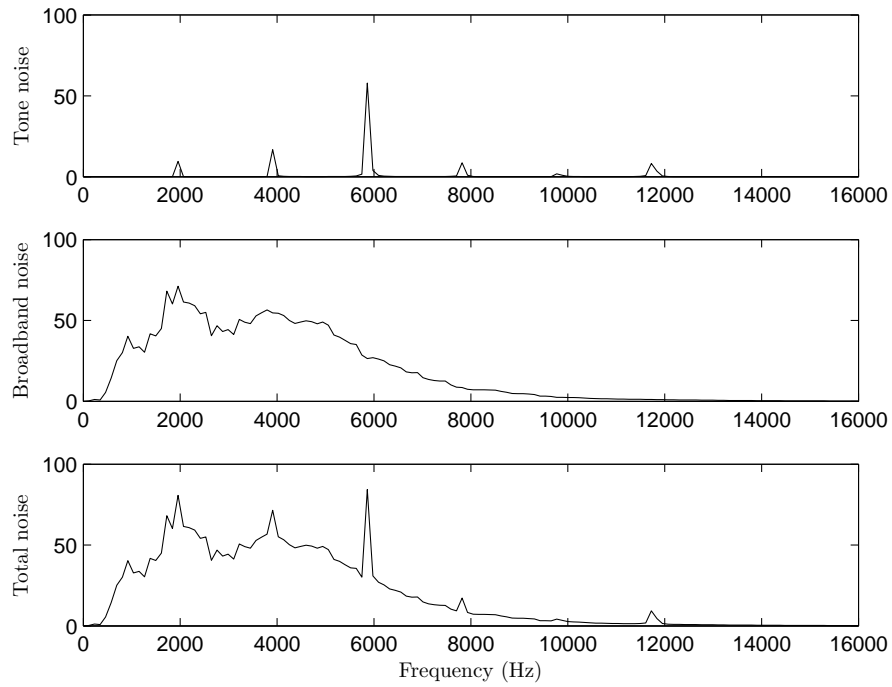


Figure 9. Power spectra of case I for tone, broadband and total noise at an observer position about one shroud diameter downstream of the stator vane at the shroud radius. The broadband noise is band-pass filtered in third octave bands.

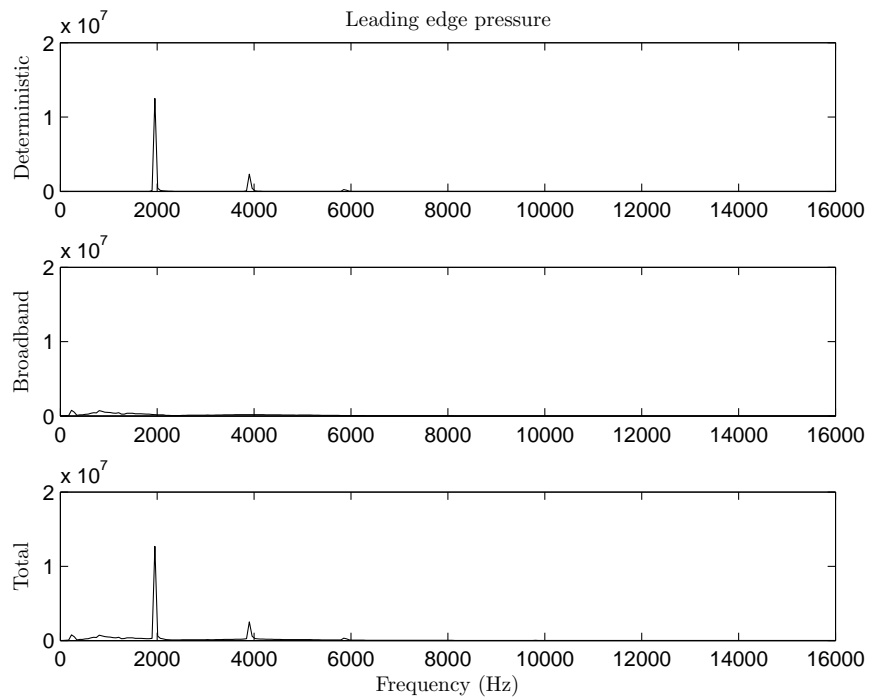


Figure 10. Power spectra at a point on the leading edge at mid radius of the mid vane of case I. The broadband part is band-pass filtered in third octave bands.

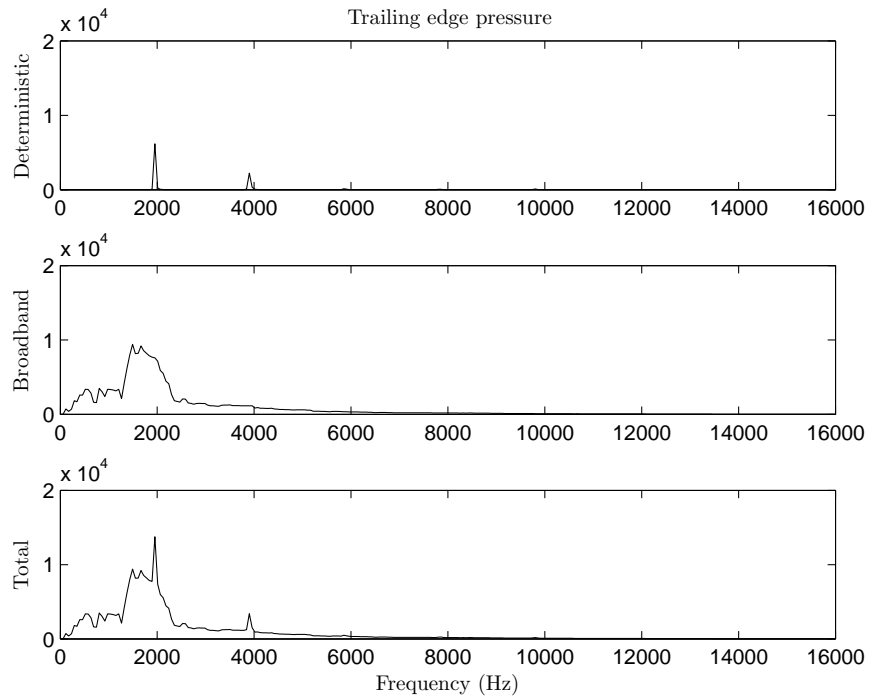


Figure 11. Power spectra at a point on the trailing edge at mid radius of the mid vane of case I. The broadband part is band-pass filtered in third octave bands.

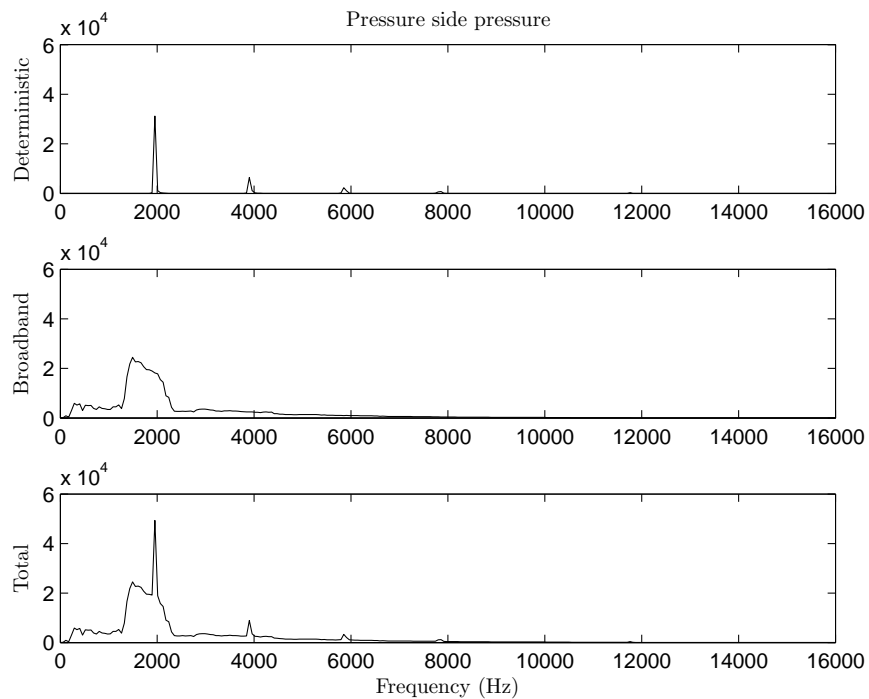


Figure 12. Power spectra at a point on the pressure side at mid radius of the mid vane of case I. The broadband part is band-pass filtered in third octave bands.

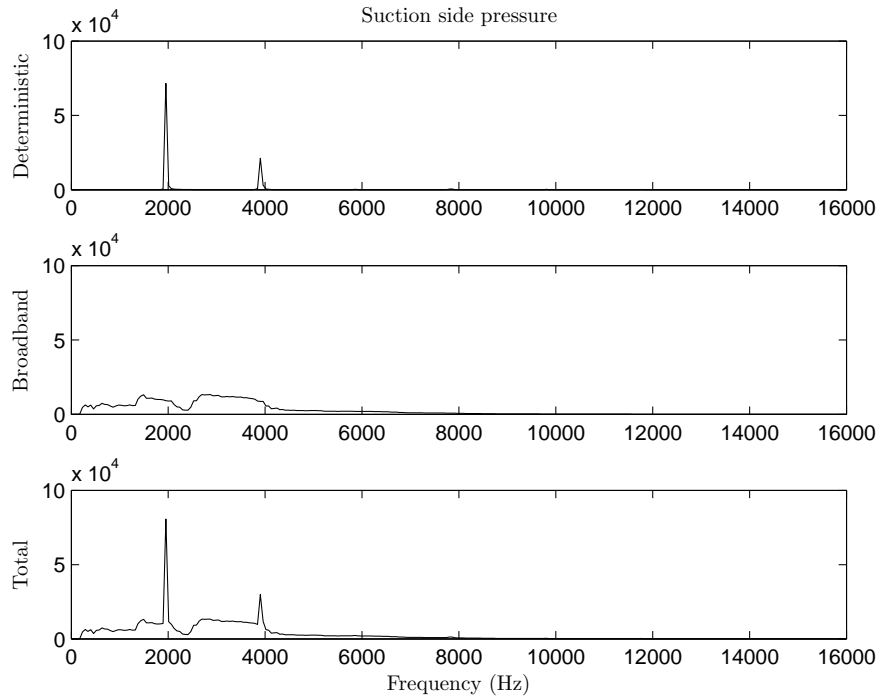


Figure 13. Power spectra at a point on the suction side at mid radius of the mid vane of case I. The broadband part is band-pass filtered in third octave bands.

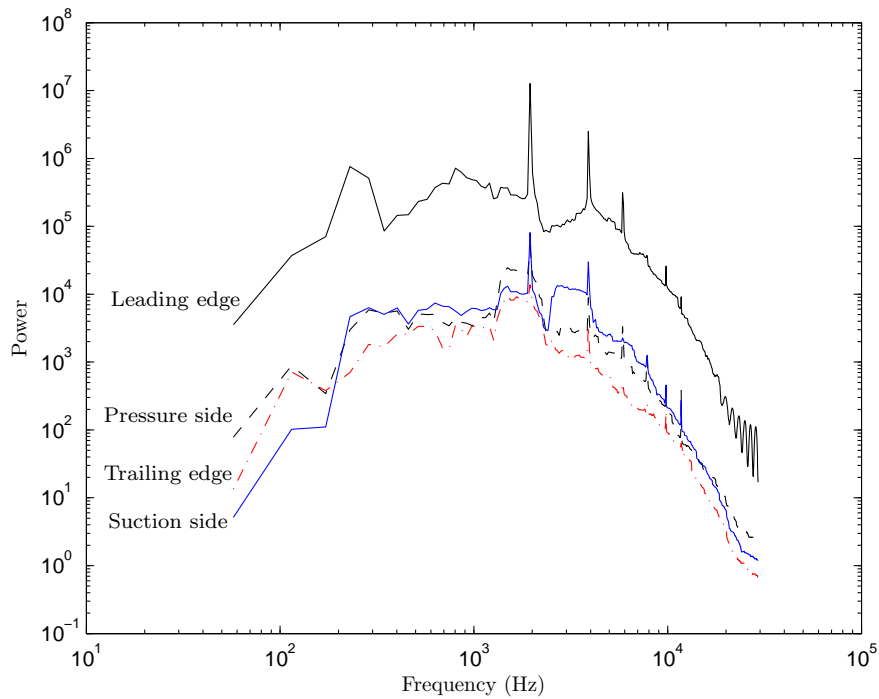


Figure 14. Power spectra at a points on the leading edge, trailing edge, pressure side and suction side at mid radius of the mid vane of case I. The broadband part is band-pass filtered in third octave bands.

cases but with a small difference at the lower frequencies. This difference should be verified by running the computation longer to obtain more samples since the accuracy of the lower frequencies are not so good (22 samples at about 2000 Hz).

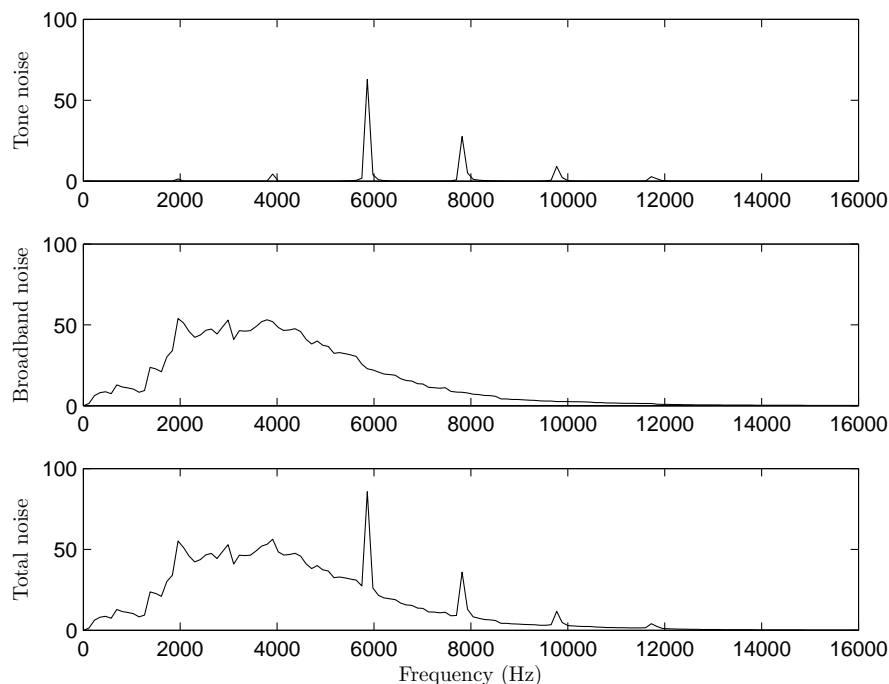


Figure 15. Power spectra of case II for tone, broadband and total noise at an observer position about one shroud diameter downstream of the stator vane at the shroud radius. The broadband noise is band-pass filtered in third octave bands.

IV. Conclusions

The method of using hybrid RANS/LES and chorochronic Buffer zones has been used for calculating both tone and broadband noise from the impingement of rotor wakes on stators. Three stator vane passages are used in the simulation to allow for some non-periodic, turbulent, behavior in the flow inside domain. Synthetic fluctuations are needed at the inlet to trigger the specified mean wake into turbulent mode. Results show that the synthetic fluctuations quickly adapt to the mean wake flow and makes it turbulent. The surface pressure of the center stator vane is sampled and analyzed and a FWH method is used to calculate the noise a bit downstream of the stator vane. Preliminary results show that a small modification of the stator blade count only have an effect on the low frequency broadband noise, but the tone noise changes a lot as expected.

Acknowledgments

This work was conducted as part of the FLOCON project (Adaptive and Passive Flow Control for Fan Broadband Noise Reduction) supported by the European Union under the Seventh Framework, Grant agreement no.: 213411. Computer time at SNIC (Swedish National Infrastructure for Computing) resources at the National Supercomputer Centre (NSC) in Linköping, Sweden, is gratefully acknowledged.

References

¹Bodony, D. J. and Lele, S. K., “Review of the Current Status of Jet Noise Predictions using Large-Eddy Simulation,” The 44th Aerospace Sciences Meeting and Exhibit, Reno, Nevada, 2006.

²Andersson, N., Eriksson, L.-E., and Davidson, L., “LES Prediction of Flow and Acoustic Field of a Coaxial Jet,” *The*

11th AIAA/CEAS Aeroacoustics Conference, No. 2884 in AIAA 2005, Monterey, California, 2005.

³Andersson, N., Eriksson, L.-E., and Davidson, L., "Effects of Inflow Conditions and Subgrid Model on LES for Turbulent Jets," *The 11th AIAA/CEAS Aeroacoustics Conference*, No. 2925 in AIAA 2005, Monterey, California, 2005.

⁴Envia, E., Wilson, A. G., and Huff, D. L., "Fan Noise: A Challenge to CAA," *International Journal of Computational Fluid Dynamics*, Vol. 18(6), 2004, pp. 471–480.

⁵Tyler, J. M. and Sofrin, T. G., "Axial Flow Compressor Noise Studies," *SAE Transactions*, Vol. 70, 1962, pp. 309–332.

⁶Gerolymos, G. A., Michon, G. J., and Neubauer, J., "Analysis and Application of Chorochnic Periodicity in Turbomachinery Rotor/Stator Interaction Computations," *J. Propulsion and Power*, Vol. 18, 2002, pp. 1139–1152.

⁷Li, H. D. and He, L., "Single-passage solution of three-dimensional unsteady flows in a transonic fan rotor," *Proceedings of the Institution of Mechanical Engineers, Part A: Journal of Power and Energy*, Vol. 215, 2001, pp. 653–662.

⁸Li, H. D. and He, L., "Single-passage analysis of Unsteady Flows around Vibrating Blades of a Transonic Fan under Inlet Distortion," *ASME Journal of Turbomachinery*, Vol. 124, 2002, pp. 285–292.

⁹Lebrun, M. and Favre, C., "Fan-OGV Unsteady Navier-Stokes Computation using an Adapted Acoustic Mesh," The 10th AIAA/CEAS Aeroacoustics Conference, Manchester, United Kingdom, 2004.

¹⁰Schnell, R., *Numerische Simulation des akustischen Nahfeldes einer Triebwerksgebläsestufe*, Ph.D. thesis, Fakultät V – Verkehrs- und Maschinensysteme der Technischen Universität Berlin, 2004.

¹¹Olausson, M., Eriksson, L.-E., and Baralon, S., "Nonlinear Rotor Wake/Stator Interaction Computations," No. 1307, The 18th ISABE meeting, Beijing, China, 2007.

¹²Olausson, M., "Turbomachinery Aeroacoustic Calculations using a Time Domain Chorochnic Method," Licentiate Thesis, Division of Fluid Dynamics, Dept. of Applied Mechanics, Chalmers University of Technology, Gothenburg, 2008.

¹³Baralon, S., Eriksson, L.-E., Billson, M., and Andersson, N., "Evaluation of Advanced Prediction Methods for Aero Engine Exhaust Noise," No. 1190, The 17th ISABE meeting, Munich, Germany, 2005.

¹⁴Jurdic, V., Moreau, A., Joseph, P., Enghardt, L., and Coupland, J., "A Comparison between Measured and Predicted Fan Broadband Noise due to Rotor-Stator Interaction," 13th AIAA/CEAS Aeroacoustics Conference, Rome, Italy, 2007.

¹⁵Li, Q., Peake, N., and Savill, M., "Large Eddy Simulations for Fan-OGV Broadband Noise Prediction," 14th AIAA/CEAS Aeroacoustics Conference, Vancouver, Canada, 2008.

¹⁶Jacob, M. C., Boudet, J., Casalino, D., and Michard, M., "A Rod-Airfoil Experiment as a Benchmark for Broadband Noise Modeling," *Theoretical and Computational Fluid Dynamics*, Vol. 19, 2005, pp. 171–196.

¹⁷Olausson, M., Eriksson, L.-E., and Baralon, S., "Evaluation of Nonlinear Rotor Wake/Stator Interaction by using Time Domain Chorochnic Solver," No. 0064, The 8th ISAIF meeting, Lyon, France, 2007.

¹⁸Davidson, L., "Using Isotropic Synthetic Fluctuations As Inlet Boundary Conditions For Unsteady Simulations," *Advances and Applications in Fluid Mechanics*, Vol. 1, No. 1, 2007, pp. 1–35.

¹⁹Eriksson, L.-E., "Development and Validation of Highly Modular Flow Solver Versions in G2DFLOW and G3DFLOW," Internal report 9970-1162, Volvo Aero Corporation, Sweden, 1995.

²⁰Eriksson, L.-E., "Private communication," Division of Thermo and Fluid Dynamics, Chalmers University of Technology, Gothenburg, Sweden, 2008.

²¹Yan, J., Mockett, C., and Thiele, F., "Investigation of Alternative Length Scale Substitutions in Detached-Eddy Simulation," *Flow, Turbulence and Combustion*, , No. 74, 2005, pp. 85–102.

²²Andersson, N., *A Study of Subsonic Turbulent Jets and Their Radiated Sound Using Large-Eddy Simulation*, Ph.D. thesis, Division of Fluid Dynamics, Chalmers University of Technology, Gothenburg, 2005.

²³Andersson, N., Eriksson, L.-E., and Davidson, L., "Large-Eddy Simulation of a Mach 0.75 Jet," *The 9th AIAA/CEAS Aeroacoustics Conference*, No. 3312 in AIAA 2003, Hilton Head, South Carolina, 2003.

²⁴Ffowcs Williams, J. E. and Hawkings, D. L., "Sound Generated by Turbulence and Surfaces in Arbitrary Motion," *Phil. Trans. Roy. Soc.*, Vol. A 264, 1969, pp. 321–342.

²⁵Brentner, K. S. and Farassat, F., "Modeling Aerodynamically Generated Sound of Helicopter Rotors," *Progress in Aerospace Sciences*, Vol. 39, No. 2-3, 2003, pp. 83–120.